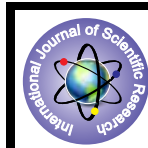


Performance of Warm Deep Drawing Process for AA1050 Cylindrical Cups with and Without Blank Holding Force



Engineering

KEYWORDS : AA1050, warm deep drawing, blank holding force, temperature, coefficient of friction, strain rate, finite element analysis.

A.Chennakesava Reddy

Professor, Department of Mechanical Engineering, JNTUH College of Engineering, Kukatpally, Hyderabad, Telangana State, India

ABSTRACT

In this paper, a statistical approach based on Taguchi techniques and finite element analysis have been adopted to determine the performance of the warm deep drawing process for AA1050 cylindrical cups drawn with and without the blank holding force. The maximum forming loads without and with the BHF, respectively are found to decrease from 1.1KN to 0.47KN and 1.5KN to 0.6KN over the working temperature range $300^{\circ}C \leq T \leq 500^{\circ}C$. No wrinkles are found till the strain reached 0.5 and 1.2 without and with the BHF respectively. The coefficient of friction all by itself contributes 87.86% of the total variation in the height of the cup drawn with BHF. The cups are drawn to the designed height (75 mm) of cup without BHF and surface expansion ratio greater than 2.0. The height of the cup drawn with the BHF is not only depended on the surface expansion ratio but also on the coefficient of friction. For the successful drawn cups, the coefficient of friction is 0.1.

INTRODUCTION

Wrinkling and tearing rupture are the common failures of deep drawing cups during the deep drawing process. The process variables, which affect the failure of the cup drawing process, include material properties, die design, and process parameters such as temperature, coefficient of friction, strain rate, blank holding force, punch and die corner radii and drawing ratio. In the deep drawing process, the formability has been improved using differential temperature rather than a uniform temperature rise as stated by Shehata et al., (1978). Furthermore, analytical models have been used by Toros et al. (2008) to evaluate the deep drawing process at elevated temperatures and under different blank holder pressure (BHP). Reddy et al. (2012) have studied the extent of thinning at punch corner radius is found to be lesser in the warm deep-cup drawing process of extra-deep drawing (EDD) steel at 200°C. Here, the warm deep drawing process of the EDD steel is carried out experimentally. In another work (Reddy, 2012) on the cup drawing process using an implicit finite element analysis, the thinning is observed on the vertical walls of the cup with high values of strain at the thinner sections. In the finite element simulations, a forming limit diagram (FLD) has been successfully applied to analyze the fracture phenomena (Marciniak & Cuczynski, 1967; Guo et al., 1990). The fracture behavior is analyzed by comparing the strain status corresponding to elements.

AA1050 aluminum alloy is not heat treatable. It is difficult to deep draw and to have minimum wall thickness of less than 1 mm. Therefore, it is expensive to exploit the combination of high strength and thin wall cups using deep drawing process. AA1050 is known for its excellent corrosion resistance, high ductility and highly reflective finish. Applications of AA1050 are typically used for chemical process plant equipment, food industry containers, architectural flashings, lamp reflectors, and cable sheathing. In the present work, the performance of warm deep drawing process is assessed during the fabrication of AA1050 cups with and without blank holding force (BHF). The design of experiments is carried out using Taguchi technique and the warm deep drawing process is executed using the finite element analysis software namely D-FORM 3D. The investigation is focused on the process parameters such as temperature, coefficient of friction, strain rate and blank holding force.

MATERIALS AND METHODS

AA1050-O was used to fabricate deep drawing cups. The tensile, yield and shear strengths of this alloy are 76, 28 and 51 MPa respectively. The elastic modulus is 69 GPa. The Poisson's ratio is 0.33. The controllable process parameters are those parameters that a manufacturer can control the design of the product, and the design of process. The levels chosen for the control parameters were in the operational range of AA1050 aluminum alloy

using deep drawing process. Each of the three control parameters was studied at three levels. The chosen control parameters are summarized in table-1. The orthogonal array (OA), L9 was selected for the present work. The parameters were assigned to the various columns of O.A. The assignment of parameters along with the OA matrix is given in table-2.

Table -1. Control parameters and levels

Factor	Symbol	Level-1	Level-2	Level-3
Coefficient of Friction	A	300	400	500
Temperature, °C	B	0.10	0.15	0.20
Strain rate, 1/s	C	100	200	300
Blank holding force (BHF), N	D	BHF-1	BHF-2	BHF-3

Table -2. Orthogonal array (L9) and control parameters

Treat No.	A	B	C	D
1	1	1	1	1
2	1	2	2	2
3	1	3	3	3
4	2	1	2	3
5	2	2	3	1
6	2	3	1	2
7	3	1	3	2
8	3	2	1	3
9	3	3	2	1

Fabrication of Deep Drawn Cups:

The blank size was calculated by equating the surface area of the finished drawn cup with the area of the blank. The diameter meter of the blank was calculated by the following equations:

$$D = \sqrt{d^2 + 4dh} \quad \text{for } d/r > 20 \quad (1)$$

$$D = \sqrt{d^2 + 4dh} - 0.5r \quad \text{for } 10 < d/r < 20 \quad (2)$$

$$D = \sqrt{d^2 + 4dh} - r \quad \text{for } 15 < d/r < 10 \quad (3)$$

$$D = \sqrt{(d - 2r)^2 + 4d(h - r) + 2\pi r(d - 0.7r)} \quad \text{for } d/r < 10 \quad (4)$$

where d is the mean diameter of the cup (mm), h is the cup height (mm) and r is the corner radius of the die (mm).

The drawing force based on the yield strength of the material was expressed by the following equation:

$$F_d = \pi dt[D/d - 0.6]\sigma_y \quad (5)$$

where D is the diameter of the blank before operation (mm), d is the diameter of the cup after drawing (mm), t is the thickness of the cup (mm) and σ_y is the yield strength of the cup material (N/mm²).

The drawing punches must have corner radius exceeding three times the blank thickness (t). However, the punch radius should not exceed one-fourth the cup diameter (d).

$$3t < \text{Punch radius} < d/4 \quad (6)$$

For smooth material flow the die edge should have generous radius preferably four to six times the blank thickness but never less than three times the sheet thickness because lesser radius would hinder material flow while excess. The corner radius of the die was calculated from the following equation:

$$r = 0.8\sqrt{(D - d)t} \quad (7)$$

The drawing ratio was roughly calculated as

$$DR = D/d \quad (8)$$

The material flow in drawing may render some flange thickening and thinning of walls of the cup inevitable. The space for drawing was kept bigger than the sheet thickness. This space is called die clearance.

$$\text{Clearance, } c = t + \mu\sqrt{10t} \quad (9)$$

Too large a blank hold force (BHF) would result in tearing along cup wall. Too low a value would lead to wrinkling in the flange. An approximate expression for holding force was given based on the initial area of the blank and the yield strength of the material.

$$BHF = \alpha\sigma_y \times \pi[D^2 - (d + 2.2t + 2r)^2] \quad (10)$$

Since AA1050 is a soft material the value of α is taken as 0.05 for BHF-1, 0.075 for BHF-2 and 0.1 for BHF-3 respectively.

Finite Element Modeling and Analysis

The finite element modeling and analysis was carried using D-FORM 3D software. The circular sheet blank was created with desired diameter and thickness. The cylindrical top punch, cylindrical bottom hollow die were modeled with appropriate inner and outer radius and corner radius. The clearance between the punch and die was calculated as in Eq. (9). The BHF was calculated using Eq. (10). The sheet blank was meshed with tetrahedral elements. The modeling parameters of deep drawing process were as follows:

- Number of elements for the blank: 21980 tetrahedron
- Number of nodes for the blank: 7460
- Top die polygons: 9120
- Bottom die polygons: 9600

The basic equations of the rigid-plastic finite element analysis were as follows:

$$p_{ij} = 0 \quad (11)$$

Compatibility and incompressibility equations:
 Strain rate tensor, $\dot{\epsilon}_{ij} = \frac{1}{2}(\dot{u}_{ij} + \dot{u}_{ji})$,
 $\dot{\epsilon}_{kk} = 0$ (12)
 where u_{ij} and u_{ji} are velocity vectors.

Constitutive equations
 Stress tensor, $\sigma_{ij} = \frac{2\mu}{3} \dot{\epsilon}_{ij}$ (13)
 where, equivalent stress, $\sigma_{eq} = \sqrt{\frac{3}{2}(\dot{\epsilon}_{ij}\dot{\epsilon}_{ij})}$ and
 equivalent strain, $\epsilon_{eq} = \sqrt{\frac{2}{3}(\epsilon_{ij}\epsilon_{ij})}$

The Coulomb's friction model was given by

$$\tau_f = \mu p \quad (14)$$

where μ is the coefficient of friction (COF), p is the normal pressure, and τ_f is the frictional shear stress.

The flow stress based on the strain hardening was computed by the following equation:

$$\sigma_f = K\epsilon^n \quad (15)$$

where, K and n are work hardening parameters depending on mechanical properties of material.

The flow stress equation considering the effects of the strain, strain rate and temperature was given by

$$\sigma_f = f(\epsilon, \dot{\epsilon}, T) \quad (16)$$

where, ϵ represents the strain, $\dot{\epsilon}$ represents the strain rate and T represents the temperature.

Johnson-Cook Model (1983) is among the most widely used mode. It connects all the deformation parameters in the following compact form.

$$\sigma_f = [\sigma + K\epsilon^n] \left[1 + S \ln \frac{\dot{\epsilon}}{\dot{\epsilon}_0} \right] \left[1 - \left(\frac{T - T_0}{T_m - T_0} \right)^m \right] \quad (17)$$

where, σ is a reference strain rate taken for normalization; σ is the yield stress and K is the strain hardening factor, whereas S is a dimensionless strain rate hardening coefficient. Parameters n and m are the power exponents of the effective strain and strain rate.

In the present work, two deep drawing processes were used. One was without blank holding die and another with blank holding die, as shown in Fig-1. The contact between blank/punch, die/blank and, blank/blank holder were coupled as contact pair. The mechanical interaction between the contact surfaces was assumed to be frictional contact and modeled as Coulomb's friction model as defined in Eq. (14). The finite element analysis was chosen to find the metal flow, effective stress, height of the cup, and damage of the cup. The finite element analysis was carried out using D-FORM 3D software according to the design of experiments.

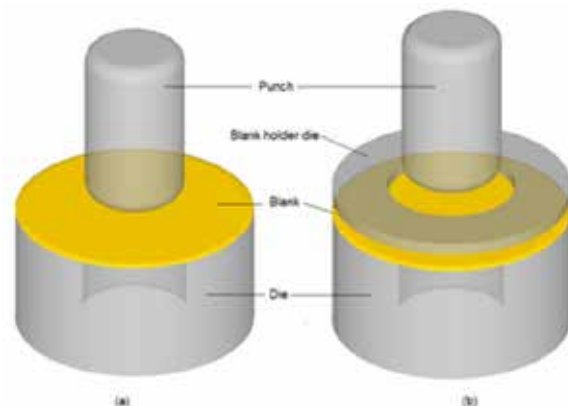


Fig-1. Two deep drawing models: (a) without blank holding die and (b) with blank holding die.

RESULTS AND DISCUSSION

Two trials were carried out with different meshes for each experiment.

Influence of process parameters on effective Stress

Table-3 gives the ANOVA (analysis of variation) summary of raw data without BHF. The Fisher's test ($F = 2.64$) is carried out on all the parameters (A, B and C) at 90% confidence level. The coefficient of friction, A contributes 23.84% of the total variation; B (temperature) gives 26.22% of the total variation; C (strain rate) puts in 22.36% of the total variation on the effective tensile stress. Fourth column of table-3 is pooled to error was no process parameter was assigned to this column. Table-4 gives the ANOVA summary of raw data with BHF. The process parameters namely coefficient of friction (A), temperature (b), strain rate (C) and blank holding force (D), respectively concede 6.84%, 24.15%, 40.95% and 27.90% of the total variation on the effective tensile stress.

Table-3. ANOVA summary of the effective stress without BHF

Source	Sum 1	Sum 2	Sum 3	SS	v	V	F	P
A	63.57	351.66	65.86	9149.03	2	4574.52	7064.90	23.84
B	360.88	65.71	54.50	10062.20	2	5031.10	7770.04	26.22
C	103.72	341.45	35.92	8581.16	2	4290.58	6626.38	22.36
Column-4 is pooled to error								
e-pool					11	5291.45		27.58
T	584.05	817.93	522.38	38375.80	17			100

Note: Note: SS is the sum of square, v is the degrees of freedom, V is the variance, F is the Fisher's ratio, P is the percentage of contribution and T is the sum squares due to total variation.

Table 4. ANOVA summary of the effective stress with BHF

Source	Sum 1	Sum 2	Sum 3	SS	v	V	F	P
A	141.61	114.99	103.15	129.33	2	64.67	36.85	6.84
B	92.75	104.99	162.01	455.45	2	227.73	129.75	24.15
C	172.80	78.70	108.25	771.93	2	385.97	219.91	40.94
D	77.99	124.75	157.01	526.19	2	263.10	149.91	27.90
e				1.76	9	0.20	0.11	0.17
T	485.15	423.43	530.42	1884.66	17			100

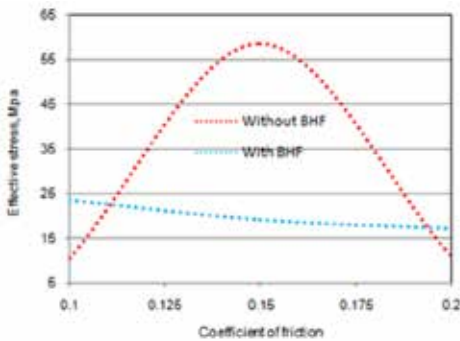


Fig-2. Influence of friction on the effective stress.

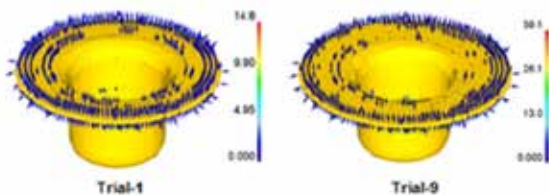


Fig-3. Normal pressure due to friction (for trials 1 and 9).

The influence of friction on the effective stress is shown Fig-2. The effective stresses of the cups drawn without BHF are found to be 10.60 MPa, 58.61 MPa and 11.00 MPa respectively for the

friction coefficient of 0.01, 0.15 and 0.20. The coefficient of friction between the blank and the blank holder is negligible, so frictional force is zero. In contrast, the effective stress of the cups drawn with BHF is decreased with an increase of friction coefficient. In this work, the coefficient of friction is varied from 0.1 to 0.2. Therefore, the shear stress due to friction varies from 0.1P to 0.2P, where P is the normal pressure. The normal pressures developed in the cup drawn under trials 1 and 9 are shown in Fig-3. The shear stresses due to friction are 1.48 and 7.82 MPa for trials 1 and 9 respectively. This increase is due to increase in real area of contact with increasing coefficient of friction (for trials 1 and 9, BHF is same). The increase in the nominal contact pressure crushes the surface asperities of the blank giving rise to more real contact area. The surface areas for trails 1 and 9 are 797.07 and 978.06 mm² respectively for the same height of the cup drawn. Hence, the result is the reduction of equivalent stress (force/area).

The effective stress is decreased from 23.60 to 17.19 MPa with increase in the temperature from 300 to 500°C (Fig-4) for the cups drawn without BHF. This is owing to the softening of material with an increase in the temperature. The maximum forming load is decreased as the working temperature increased. The maximum forming load without BHF is found to decrease from 1.1kN to 0.47kN over the working temperature range 300°C ≤ T ≤ 500°C as shown in Fig-5. The effective stress increases with an increase of temperature for the cups drawn with BHF even though the maximum forming load with BHF is found to decrease from 1.5kN to 0.6kN over the working temperature range 300°C ≤ T ≤ 500°C. This may be due to the strain hardening of the blank material as implied from Eqs. 16 and 17.

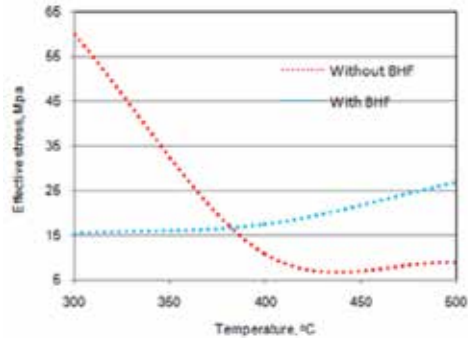


Fig-4. Influence of temperature on the effective stress.

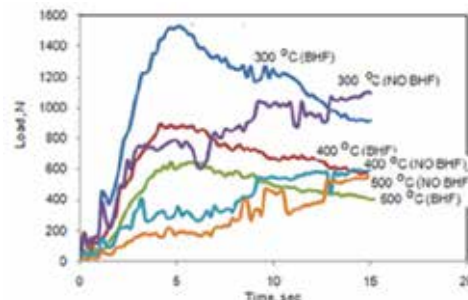


Fig-5. Effect of temperature on drawing load.

The influence of strain rate on the effective stress is shown Fig-6. The effective stresses of the cups drawn without BHF are found to be 17.29 MPa, 56.91 MPa and 5.99 MPa respectively for the strain rate of 100, 200 and 300. Till the strain reached 0.5, the major strain is equal to minor strain (ε), as depicted from Fig-7. This indicates that the material undergoes the deep drawing process. When the strain exceeded 0.5 the material suffers with wrinkling as shown in Fig-7. The effective stress of the cups

drawn with BHF is found to be 28.80 MPa, 13.12 MPa and 18.04 MPa respectively for the strain rate of 100, 200 and 300. Till the strain arrived at 1.2, the major strain is equal to minor strain (). This indicates that the material experiences the deep drawing process only without forming wrinkles as shown in Fig-8.

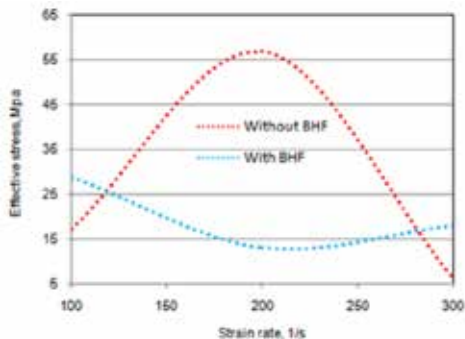


Fig-6. Influence of strain rate on the effective stress.

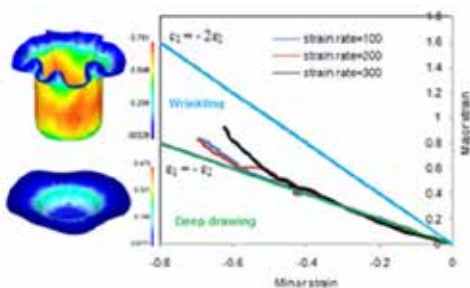


Fig-7. Forming limit diagram without BHF.

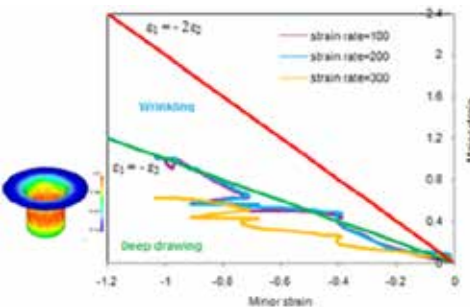


Fig-8. Forming limit diagram with BHF.

The influence of BHF on the effective stress is shown in Fig-9. The effective stress increases with an increase in the blank holding force. The force exerted by the blank holder on the blank supplies a restraining force which may detain the metal flow. This restraining action is largely applied through friction. The resultant effect is the increase of drawing force, consequently an increase in the effective stress.

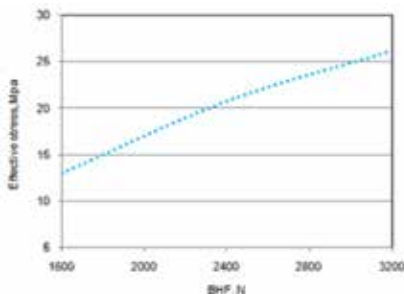


Fig-9. Influence of BHF on the effective stress.

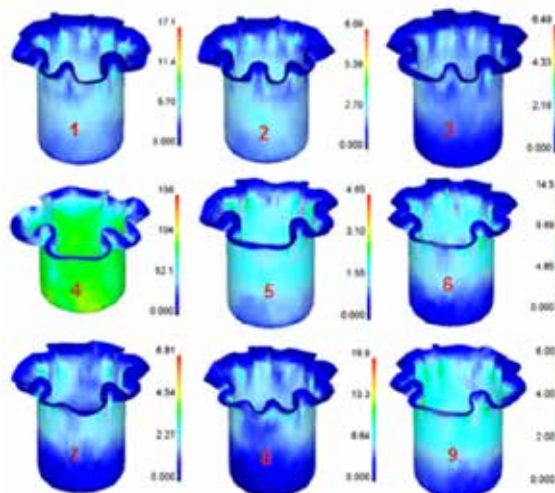


Fig-10. Influence of process parameters without BHF on the effective stress.

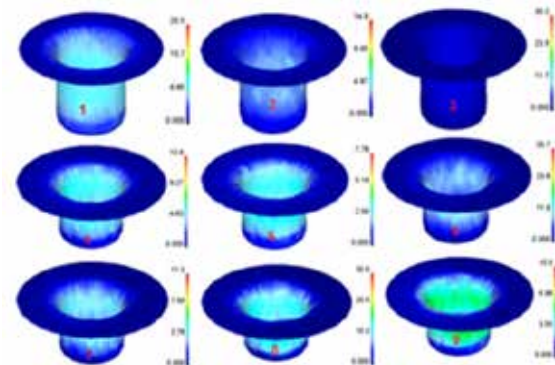


Fig-11. Influence of process parameters with BHF on the effective stress.

The FEA results of effective stress are shown in Figs-10 & 11 for various test conditions without BHF and with BHF respectively as per the design of experiments. It is found that the effective stress (156 MPa) has exceeded the yield strength (28MPa) of the AA10550 for the trail- 3 without BHF. It is also found that the effective stresses (35.2, 35.7 and 29 MPa) have exceeded the yield strength of the AA10550 for the trails- 3, 6 and 8 with BHF. In rest of the trials with or without BHF the effective stress is lower than the yield strength.

Influence of Process Parameters on Cup Height

The ANOVA summary of cup height is given in table-5. As per the Fisher's test (F = 2.64) the coefficient of friction, temperature and strain rate, respectively contribute 27.30%, 25.23% and 23.42% of the total variation without BHF. The coefficient of friction all by itself gives 87.86% of the total variation with BHF. The other variables are insignificant (table-6).

Table-5. ANOVA summary of the height of cup without BHF

Source	Sum 1	Sum 2	Sum 3	SS	v	V	F	P
A	452.02	409.17	448.92	190.32	2	95.16	22.57	27.3
B	410.18	450.37	449.56	175.92	2	87.96	20.86	25.23
C	449.34	411.14	449.63	163.37	2	81.68	19.37	23.42

Column-4 is pooled to error

e-pool					11	80.38	0.11	24.05
T	1761.97	1718.91	1759.56	693.66	17			100

Table-6. ANOVA summary of the effective stress with BHF

Source	Sum 1	Sum 2	Sum 3	SS	v	V	F	P
A	452.53	381.75	328.87	1283.21	2	641.61	7.85	87.86
B	383.95	381.42	397.78	25.85	2	12.93	0.16	0.53
C	389.51	379.28	394.36	19.75	2	9.88	0.12	0.11
D	389.11	396.32	377.72	29.31	2	7.33	0.089	0.77
e				81.70	9	11.67	0.14	10.73
T	1615.1	1538.77	1498.73	1439.82	17			100

The influence of friction on the cup height is shown Fig-12. The cup heights without BHF are found to be 75.34 mm, 68.20 mm and 74.82 mm respectively for the friction coefficient of 0.1, 0.2 and 0.3. The cup height is decreased with an increase in the coefficient of friction with BHF as shown Fig-12. The cup height is increased with an increase in the temperature without BHF, as shown in Fig-13. The cup heights without BHF are found to be 74.89 mm, 68.52 mm and 74.93 mm respectively for the strain rate of 100, 200 and 300 as shown in Fig-14. The cup heights with BHF are found to be 64.91 mm, 63.21 mm and 65.73 mm respectively for the strain rate of 100, 200 and 300 as shown in Fig-14.

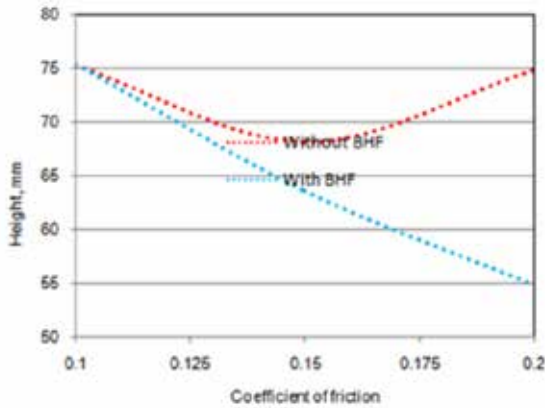


Fig-12. Influence of friction on the height of cup.

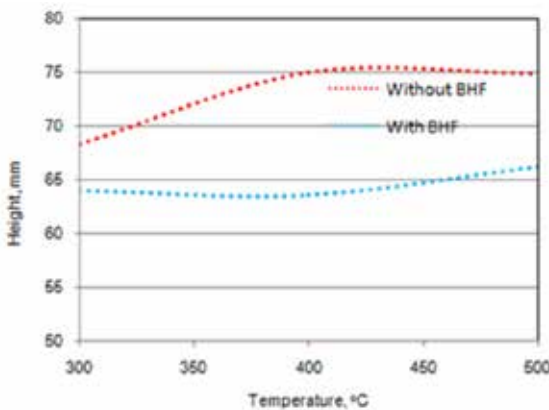


Fig-13. Influence of temperature on the height of cup.

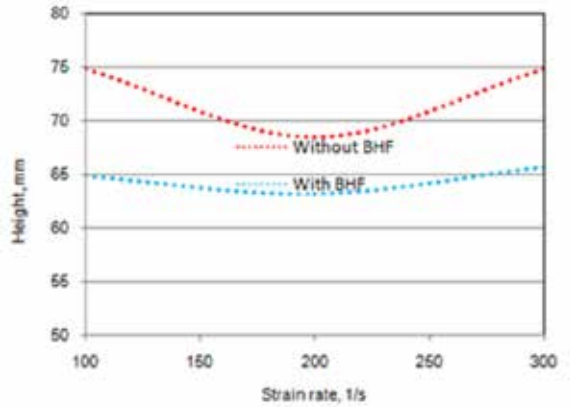


Fig-14. Influence strain rate on the height of cup.

The wrinkling is started in the cups after about 5 seconds of deep drawing process without BHF as shown in Fig-15. The cup drawn with trial 4 is only ruptured after achieving the cup height of 55.37 mm. In all other cases without BHF, there is wrinkling in the cups. With BHF the cups drawn with trials 4 to 9 are ruptured nearly 10 seconds of deep drawing process, as shown in Fig-16. Only three cups of full depths are able to get with trials 1 to 3. The major influential characteristic of the material is the ductility. The surface expansion ratio represents the ductility of the material in the deep drawing process. In the case of deep drawing process without BHF, the cups which are having surface expansion ratio greater than 2.0 were drawn to the designed height (75 mm) of cup, as shown in Fig-17. The cup height with trial 3 is 55.37 mm with surface expansion ratio of 1.71. This simple phenomenon cannot be applied to the case of deep drawing with BHF. The cups drawn with BHF are nearly having the same surface expansion ratio of 3.10, but the cups drawn with conditions of trials 4 to 9 are not reached the designed height of 75 mm as shown in Fig-18. Hence, the height of the cup drawn is not only depended on the surface expansion ratio but also on the coefficient of friction as shown in Fig-12. The cups drawn with conditions of trials 1 to 3, the designed height is reached, because the coefficient of friction is 0.1. The cups drawn with conditions of trials 4 to 9, the designed height is not reached, because the coefficient of friction is 0.2 or 0.3.

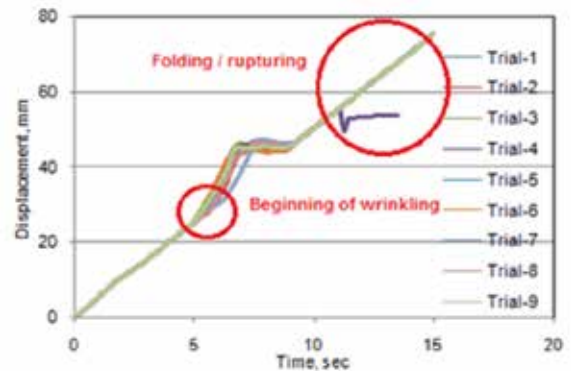


Fig-15. Displacement of cups without BHF.

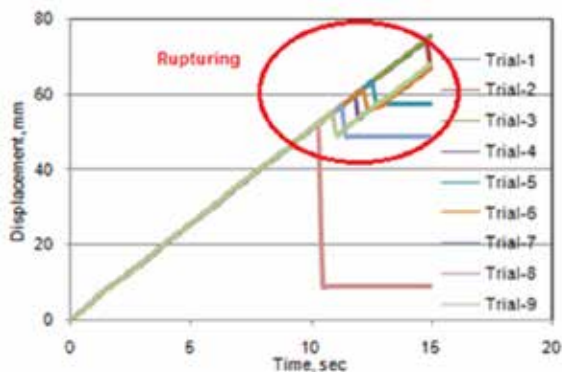


Fig-16. Displacement of cups with BHF.

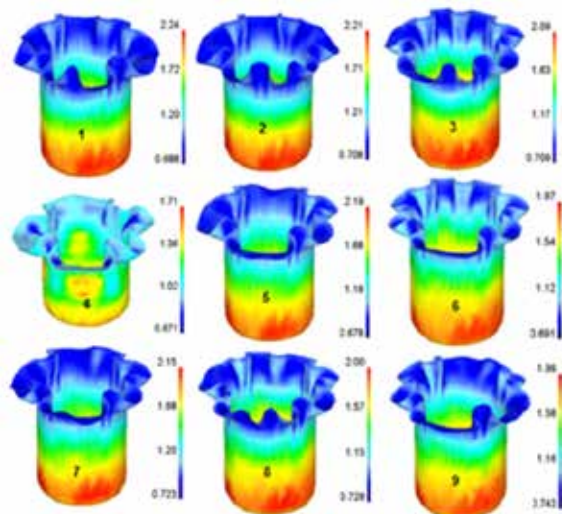


Fig-17. Surface expansion ratio of cups without BHF.

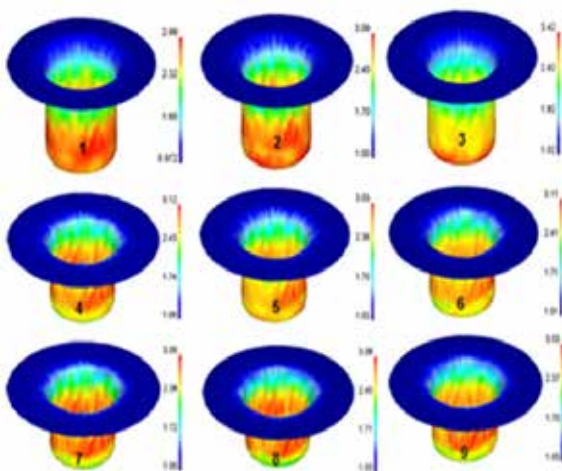


Fig-18. Surface expansion ratio of cups with BHF.

Influence of Process Parameters on Damage of Cup

The ANOVA summary of damage of cups without BHF is given in table-7. When the Fisher's test (2.64) is applied to ascertain the influence of process parameters without BHF it is found that the coefficient of friction (A), temperature (B) and the strain rate (C), respectively contribute (34.28%), 9.25% and 46.25% of the total variation. The ANOVA summary of damage of cups with BHF is given in table-8. With BHF, it is also found that the coefficient

of friction (A), strain rate (C) and BHF, respectively contribute 37.87%, 23.19% and (30.91%) of the total variation. The influence of temperature (B) is negligible.

Table-7. ANOVA summary of damage of the cups without BHF

Source	Sum 1	S u m 2	S u m 3	SS	v	V	F	P
A	4.09	6.37	3.90	0.63	2	0.31	38.76	34.28
B	5.60	4.46	4.30	0.17	2	0.09	11.25	9.25
C	3.70	6.62	4.03	0.85	2	0.42	52.52	46.25
Column-4 is pooled to error								
e-pool					11	0.09	11.25	10.22
T	17.84	21.76	17.85	1.84	17			100

Table-8. ANOVA summary of damage of the cups with BHF

Source	Sum 1	S u m 2	S u m 3	SS	v	V	F	P
A	5.43	7.82	6.90	0.49	2	0.25	10.47	37.87
B	7.28	6.51	6.35	0.08	2	0.04	1.67	6.18
C	6.07	7.80	6.27	0.30	2	0.15	6.28	23.19
D	7.56	7.12	5.46	0.40	2	0.20	8.37	30.91
e				0.02	9	0.00	0.00	1.85
T	26.33	29.25	24.99	1.29	17			100

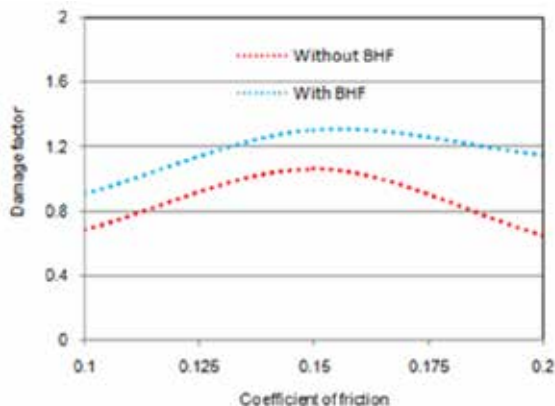


Fig-19. Influence friction on the damage of cup.

The effect of friction on the damage of cup is shown in Fig-19. Without BHF, the damage of cup is increased with the friction coefficient from 0.10 to 0.15 and it is decreased with the friction coefficient from 0.15 to 0.20. The same kind of trend is observed in the presence of the blank holding force (BHF) too. In the case of friction between the blank and the tool, the increase of the coefficient of friction determines the wrinkling to reduce, but high values of the coefficient may cause cracks and material breakage (Hedworth & Stowell, 1971). The damage is decreased with the increase of temperature as shown in Fig-20. In the presence of BHF, the effect of temperature is additional to the damage of cups. On account of temperature the material becomes soft. Because of the constraint to the material for its free movement in the presence of blank holding force, the material experiences large plastic deformation and there upon the damage of the material. The damage is found to be maximum with strain rate of 200 1/s as seen from Fig-21. The damage is decreased with the increase of BHF, as seen from Fig-22. The main reasons for the damage of cups may be due to ironing, folding, wrinkling and tearing in the absence of blank holding force.

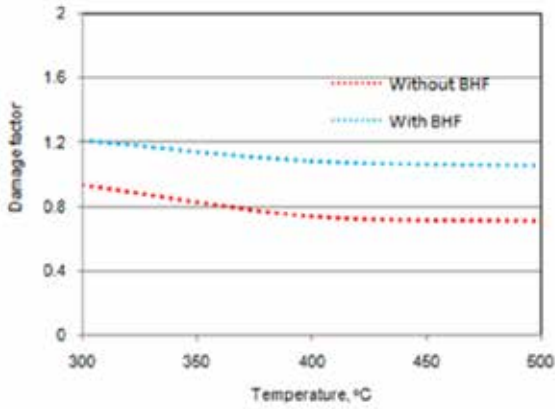


Fig-20. Influence of temperature on the damage of cup.

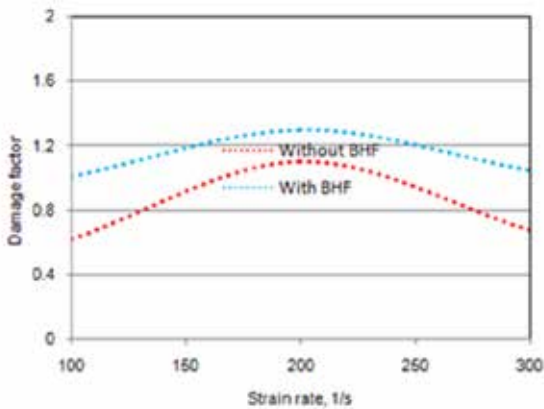


Fig-21. Influence of strain rate on the damage of cup.

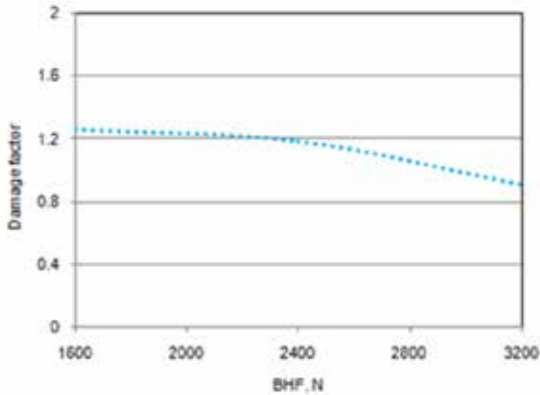


Fig-22. Influence of BHF on the damage of cup.

The contour plots of the von Mises stresses (Fig-10) shows that the portion subjected to forming without BHF experienced a stress of magnitude ranging from 6 MPa to 17 MPa. The initial yield stress of the material is 28 MPa; the above values of stress indicate that the material undergoes the elastic deformation. In case of trial 4 without BHF, the von Mises stress is 156 MPa; this value indicates that the material experiences the plastic deformation and broken after exceeding the ultimate strength (76 MPa) of the material. The contour plots of the von Mises stresses (Fig-11) shows that the portion subjected to forming with BHF experienced a stress of magnitude ranging from 7.8 MPa to 35.7 MPa. The cups drawn with the BHF under trials 1, 2, 4, 5, 7 and 9, the von Mises stresses are in the range of 7.8 to 20.8 MPa. Therefore, the cups drawn under these trials have undergone the elastic deformation and the remaining cups are

with the plastic deformation. From Fig-5 it is observed that the punch force required being more when the BHF is assumed to depend on both the normal loading and stretching phenomena. It is observed that the value of fractional real contact area between the blank and the die is increased as the nominal contact pressure increased. The increase in the nominal contact pressure crushes the surface asperities in the blank giving rise to more real contact area. The BHF is an important parameter in deep drawing process. It is used to suppress the formation of wrinkles that can appear in the flange of the drawn part. When increasing the BHF, stress normal to the thickness increases restraining any formation of wrinkles. However, the large value of the BHF may cause fracture at the cup wall.

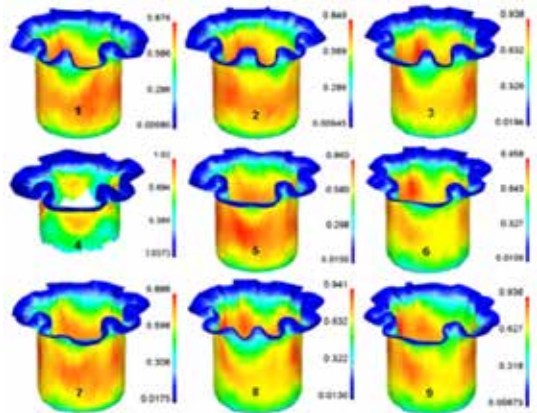


Fig-23. The damage and maximum principal strains of cups without BHF.

In the flange area, the maximum principal strain without BHF in wrinkling is smaller than that in successful drawn cups, as shown in Fig-23. While the maximum principal strain in fracture (trial 4) is much larger than that in successful drawn cups at the punch fillet radius. In consideration of the influence of a blank holder force, two main failure modes (fracture and wrinkling) are predicted in simulations. In the flange area, the maximum principal strain with BHF in wrinkling is smaller than that in fracture and successful drawn cups, as shown in Fig-24. The failure modes are judged from the height of cups drawn and the coefficient of friction. As shown in figure 16, the fracture is occurred when the cup height is in the range of 52.12 mm to 63.33 mm with coefficient of friction in the range of 0.15 and 0.20. The only process that influences the height of cup is the coefficient of friction as seen from table 6. The fracture area is located at the punch fillet radius and the die corner radius as shown in Fig-25. In the case of successful drawn cups, the coefficient of friction is 0.1 (trials 1, 2 and 3). No wrinkling is found in the cups drawn with BHF. The normal stress induced due to BHF in the thickness direction of blank suppresses the formation of wrinkles. In the absence of BHF the folding of the blank and thus wrinkling occurs in the cups, as shown in Fig-25. Due to over folding the material cannot flow into the die, thus leading the fracture of cup at the punch fillet radius in the case of trial 4 without BHF.

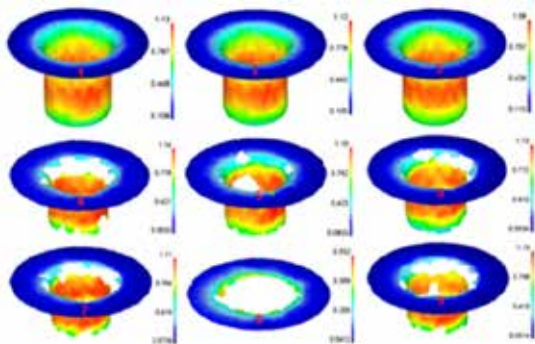


Fig-24. The damage and maximum principal strains of cups with BHF.

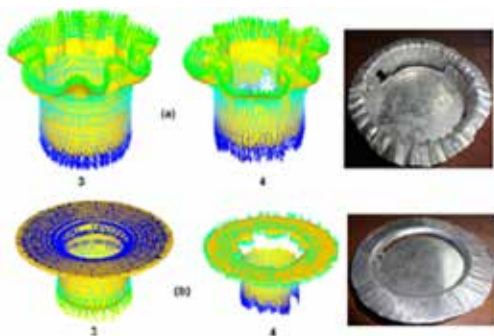


Fig- 25. Metal flow and fracture: (a) without BHF and (b) with BHF.

CONCLUSIONS

The effective stress of the cups drawn decreases with an increase of friction coefficient with the BHF. The increase in the nominal contact pressure crushes the surface asperities of the blank giving rise to more real contact area. The maximum forming loads without and with the BHF, respectively are found to decrease from 1.1kN to 0.47kN and 1.5kN to 0.6kN over the working temperature range $300^{\circ}\text{C} \leq T \leq 500^{\circ}\text{C}$. No wrinkles are found till the strain reached 0.5 and 1.2 without and with the BHF respectively. The coefficient of friction all by itself contributes 87.86% of the total variation in the height of the cup drawn with BHF. The wrinkling is started in the cups after about 5 seconds of deep drawing process without BHF. With the BHF the cups drawn are ruptured nearly 10 seconds of the deep drawing process. In the case of deep drawing process without BHF, the cups, which are having surface expansion ratio greater than 2.0, are drawn to the designed height (75 mm) of cup. The height of the cup drawn with the BHF is not only depended on the surface expansion ratio but also on the coefficient of friction. In the case of successful drawn cups, the coefficient of friction is 0.1.

ACKNOWLEDGMENT

The author wishes to thank University Grants Commission (UGC), New Delhi, India for financial assisting this project.

REFERENCE

- Guo, Y.Q., Batoz, J.L. and Detraux, J.M. 1990. Finite Element Procedures for Strain Estimations of Sheet Metal Forming Parts. *International Journal of Numerical Methods and Engineering*, 30:1385-1401. Hedworth, J. and Stowell, M.J. 1971. The measurement of strain-rate sensitivity in superplastic alloys. *Journal of Materials Science*, 6:1061-1069. Johnson, G.R. and Cook, W.H. 1983. A constitutive model and data for metals subjected to large strains, high strain rates and high temperatures. In: *Proceedings of the Seventh Symposium on Ballistics*; The Hague, The Netherlands, 1-7. Marciniak, Z. and Cuczynski, K. 1967. Limit strains in the processes of stretch-forming sheet metal. *International Journal of Mechanical Sciences*, 9(9):613-620. Reddy, A.C., Reddy, T.K.K. and Vidya Sagar, M. 2012. Experimental characterization of warm deep drawing process for EDD steel. *International Journal of Multidisciplinary Research & Advances in Engineering*, 4(3):53-62. Reddy, A.C. 2012. Evaluation of local thinning during cup drawing of gas cylinder steel using isotropic criteria. *International Journal of Engineering and Materials Sciences*, 5(2):71-76. Shehata, F., Painter, M.J. and Pearce, R. 1978. Warm forming of aluminum/magnesium alloy sheet. *J Mech Working Technol*, 2(3):279-291. Toros, S., Ozturk, F. and Ilyas Kacar. 2008. Review of warm forming of aluminum-magnesium alloys. *Journal of Materials Processing Technology*, 207(1-3):1-12.